MIJST
MIST International Journal of Science and Technology

Characterization of Mechanical Properties of Concrete Recycled Ceramic and Glass Powder Exposed to Elevated Temperatures

Tanvir Mustafy[1*], Md. Maruf Hasan[2], Nayeem Ahmed Shuvo[3], and Joarder Md Sarwar Mujib[4]

[1,2,3,4]Department of Civil Engineering, Military Institute of Science and Technology, Dhaka, Bangladesh
[1]Department of Civil Engineering, University of Alberta, Canada

emails: [1]*mustafy@ualberta.ca*; [2]*marufhasan85611@gmail.com*; [3]*nayeemahmedshuvo@gmail.com*; and [4]*maj.sarwar@ce.mist.ac.bd*

ARTICLE INFO

Article History:

Received: 24th March 2022
Revised: 08th May 2022
Accepted: 08th May 2022
Published online: 26th June 2022

Keywords:

Ceramic recycled aggregate
Glass recycled aggregate
Volumetric replacement of sand

ABSTRACT

Systematic reuse of industrial debris is a crucial component that helps shape the sustainable construction system and green technology. The effective optimization of waste ceramic and glass fines into concrete mixes, as partial replacements of natural sand by volume, has been used in this study to explore the mechanical properties of ceramic recycled aggregate (CRA) and glass recycled aggregate (GRA) concrete at higher temperatures. The study comprises 17 types of concrete mixtures comprised of normal concrete (NC) along with 8 different mixes from both GRA and CRA concrete. In both types of GRA and CRA concrete, the sand replacement (by volume) ratios are similar. This paper highlights NC along with the volumetric replacements of sand as 5%, 10%, 15%, 20%, 25%, 30%, 35%, and 40% in other mixes. A total of 306 cylinders were made whereas 18 cylinders for NC and each group (GRA and CRA) included n=18 cylinders. Selected temperatures were 25°C, 100°C, 200°C, 400°C, 600°C, and 800°C to determine the overall mechanical and chemical alterations in NC and recycled concrete. The study reveals that increasing the addition of recycled glass and ceramic fines improves the overall compressive strength, and tensile strength compared to normal concrete. Higher replacement of ceramic and glass fines reduces the cracks and enhances the durability of concrete. In addition, more strength reduction was noticed in NC with increasing temperatures, while the reduction rate was slower in both GRA and CRA concrete. Furthermore, the study expounds that, by exploiting the ceramic and glass wastes (as fines) into concrete would result in two-way environmental advantages. One is, it would reduce the hazardous ceramic and glass landfills while the other is, it would minimize the frequency of sand mining.

1. INTRODUCTION

Researchers all around the globe were urged to explore for and use more sustainable resources in response to the growing interest in sustainable development. Industrial ceramic and glass debris inclusion in the concrete could be the alternative choices for achieving sustainability in construction systems worldwide, thus removing hazardous waste from the environment. About 22 billion tons of ceramic waste powder (CWP) are produced and disposed to the environment (El-Dieb, Taha, & Abu-Eishah, 2019). It has been approximated that around 30% of ceramic waste is produced from the ceramic industry every day (Al Bakri *et al.*, 2013). Annually, the ceramic industry of India produces 100 million tons of ceramic and it contributes 15-30% of the ceramic waste to the environment (Raval, Patel, & Pitroda, 2013, Mujib *et al.*, 2022). The total quantity of glass garbage created in the European Union in 2014 was close to 18.5 million tons. A large proportion of glass debris is deposited daily and every year, almost 10 million tons of glass garbage are produced throughout the world (Salem, Khedawi, Baker, & Abendeh, 2017). According to the United Nations, the annual volume of garbage created throughout the world is 200 million tons, with glass waste accounting for 7% (Rashid et al., 2018; Topçu & Canbaz, 2004). Materials such as crushed glass or crushed concrete, which are claimed to be potential sources of environmental hazard, could be incorporated with concrete to check the fire resistivity.

Recycled ceramic wastes have been found to have a favourable influence on compressive strength, capillary absorption, alkali-silica response, freeze-thaw durability, and impermeability in tests using ceramic wastes in concrete mixtures (M. C. Bignozzi & Saccani, 2012; de Brito, Pereira, & Correia, 2005; Higashiyama, Yamauchi, Sappakittipakorn, Sano, & Takahashi, 2013; Lopez, Llamas, Juan, Moran, & Guerra, 2007; César Medina, de Rojas, & Frías, 2013; Pacheco-Torgal & Jalali, 2010; Senthamarai, Manoharan, & Gobinath, 2011, Mustafy *et al.*, 2020). Portland concrete and fly ash concrete compositions with earthenware fine recycled ceramic aggregate have increased compressive strength(Torkittikul & Chaipanich, 2010). The pozzolanic activity of recycled coarse sanitary ware ceramic aggregate boosted concrete samples' compressive strength (C. Medina, Sánchez de Rojas, & Frías, 2012). Concrete with both coarse and fine sanitary ware aggregate has greater compressive strength and is more resistant to temperature increases (Halicka, Ogrodnik, & Zegardlo, 2013). They found that the aggregate in sanitary ware was mostly made up of SiO_2 (65.80 percent), Al2O3 (22.20%), with traces of K_2O (3.50%), and Na_2O. (1.25%). A blend of waste ceramic powder (WCP) and alkali-activated mortars demonstrate a considerable improvement in concrete construction resistance capability up to 950°C (Huseien et al., 2018). The most common oxides found in ceramic aggregate made from an electoral insulator are SiO2 (70.90%), Al_2O_3(21.10%), and traces of K_2O (3.57%) and Na_2O (1.47%) (Higashiyama, Sappakittipakorn, Mizukoshi, & Takahashi, 2014). Due to the probable pozzolanic effect of ceramic waste, they found that using fine ceramic aggregate based on electrical insulators increases compressive strength.

Container-derived recycled glass has been utilized as fine aggregate in concrete (Corinaldesi, Gnappi, Moriconi, & Montenero, 2005; de Castro & de Brito, 2013; Jin, Meyer, & Baxter, 2000; Shao, Lefort, Moras, & Rodriguez, 2000). Crushed waste glass materials, as a 30% replacement of sand, were found to provide greater compressive strength than conventional concrete (Adaway & Wang, 2015). Because of the near-zero porosity and non-hydrophilic character of glass, incorporating it into mortar and concrete has several advantages, including greater workability, improved resistance to chloride ion penetration, and reduced drying shrinkage (Chen, Chang, Wang, & Huang, 2011; Topcu & Canbaz, 2004). The molten crushed glass fills the inner voids in concrete (above 600°C) and thus major contributions to the water sorptivity and porosity (Ling, Poon, & Kou, 2012). The larger the amount of waste glass used to replace aggregates, the longer the initial and final setting durations. At temperatures above 150°C, concrete containing 10% waste glass as an aggregate has better compressive strength than regular concrete (Terro, 2006). The main disadvantage is the poor bonding between the smooth glass surface and the cement hydration products (Al-Sibahy & Edwards, 2012; Park, Lee, & Kim, 2004), as well as the possibility of detrimental expansion owing to the alkali-silica reaction (ASR), which occurs slowly between silica-rich glass aggregate and alkali in the cement paste. The latter issue, on the other hand, can be addressed by using mineral additions having pozzolanic properties (Liu, 2011). In addition, certain research investigations on the usage of recycled glass (RG) as a pozzolanic material for cement substitution were done (Federico & Chidiac, 2009; Oliveira, de Brito, & Veiga, 2015). RG must be crushed into a powder with a particle size of fewer than 150 μm in order to initiate the pozzolanic reactivity (Y.-c. Guo, Zhang, Chen, & Xie, 2014; Schwarz, Cam, & Neithalath, 2008; Shi, Wu, Riefler, & Wang, 2005, Mustafy & Ahsan, 2010).

High temperatures experienced in fires can exacerbate the component loss of bearing capacity, significantly erode mechanical qualities, jeopardize building structural safety, and potentially cause building collapse (Holan, Novak, Müller, & Štefan, 2020; L.-J. Li, Xie, Liu, Guo, & Deng, 2011; M. Li, Qian, & Sun, 2004; W. Li, Wang, & Han, 2019). Material changes such as cracking pattern, deformation, and discoloration must be visually noticed for this purpose, and non-destructive tests and core tests must be performed to quantify the concrete's deterioration degree, such as strength decrease and counterbalance (Colombo & Felicetti, 2007; Dilek, 2005; Dos Santos, Branco, & de Brito, 2002; Lee, Choi, Hong, & Engineering, 2009). At 400°C, the concrete's residual compressive strength appears to drop by 60%, and at 800°C, it is below 10% (Lee et al., 2009). Throughout the fire episode, temperatures in buildings may reach 1100°C and even 1350°C in tunnels, causing significant damage to concrete structures (38, 2007; Hager, 2013). Furthermore, according to a literature review, concrete loses around 25% of its compressive strength when heated to 300°C, and about 75% when heated to 600°C (G. Khoury, 1992; Lankard, Birkimer, Fondriest, & Snyder, 1971). When heated to 300 °C, normal strength concrete (NSC) generally loses 10 to 20% of its initial compressive strength, and 60 to 75% when heated to 600°C. In a similar way, elastic modulus falls. At temperatures below 450°C, increased rates of strength loss, up to 40% of initial strength, were recorded for high strength concrete (HSC) (Phan & Carino, 2000). Concrete turns pink or red at temperatures ranging from 300°C to 600°C, whitish-grey at temperatures ranging from 600°C to 900°C, and brownish yellow color at temperatures ranging from 900°C to 1000°C (Lee et al., 2009). We can determine the extent of compressive strength deterioration by monitoring the color shift because the concrete's color value changes as temperature rises (Georgali & Tsakiridis, 2005; Short, Purkiss, & Guise, 2001). The structural performance of reinforced concrete construction, which accounts for a substantial fraction of structures, is damaged during a building fire, structural deformation rises, and load-carrying capacity decreases (Dong, Cao, Bian, & Zhang, 2014).

Dissociation of $Ca(OH)_2$ at 300ºC-400°C, large and rapid creep, generally resulting in failure at 600°C, dissociation of $CaCO_3$ at 700°C, ceramic binding and total water loss at

800°C, and melting at 1200-1350°C were evaluated (G. A. J. P. i. s. e. Khoury & materials, 2000; Sarker, Kelly, & Yao, 2014). It was observed that, between 500 and 600°C, Ca(OH)2 dehydrates (Heikal, 2000). It has been investigated the effects of chilling on concrete (G. A. Khoury, Grainger, & Sullivan, 1986). Cooling strains (shrinkage) were discovered to be a result of the aggregate cement interaction, which causes cracking, and were unrelated to the concrete's age, initial moisture content, or heating rate. Spalling of concrete was effectively exhibited to be declined from 22% to less than 1% when polypropylene fibers (3 kg/m^3) were utilized in the concrete (Ali, Nadjai, Silcock, & Abu-Tair, 2004).

The post-fire performance regimes of concrete structures using alkali-activated fly ash cement have been exhibited to be severely dropped at successively higher temperatures i.e. 600°C to 700°C (Fernández-Jiménez, Pastor, Martín, & Palomo, 2010). Concrete incorporated with pozzolanic components such as metakaolin, inflated strength up to 200°C and sustained greater strengths up to 400°C than fly-ash, silica fume, and standard Ordinary Portland Cement (OPC) concrete (Poon, Azhar, Anson, & Wong, 2003). The effect of elevated temperature heat and strain rate on the residual strength of ternary blended concrete containing fly ash and silica fume was investigated (Z. Li, Xu, & Bai, 2012). After the fire episode of 400°C on concrete, there was a significant loss of strength whereas all of the high-strength-concretes (HSC) quickly deteriorated at 400°C. There have been numerous investigations pivoting on the fire performance of concrete components. After 10 minutes at 800°C, it was observed that a 25% loss in compressive strength of 25 mm cube metakaolin-based geopolymer paste specimens (D. L. Y. Kong, Sanjayan, & Sagoe-Crentsil, 2005). The strength of a fly ash-based geopolymer paste increased by 6% following exposure to the heat of 800°C (D. L. Kong, Sanjayan, & Sagoe-Crentsil, 2007).

Metallic fiber reinforced concrete, when exposed to fire episodes, they have a favourable effect, enhancing energy absorption and minimizing cracking (Bednář, Wald, Vodička, & Kohoutková, 2013; Fike & Kodur, 2011; Kim & Lee, 2015). Because of the physical and mechanical qualities of polypropylene fibers, concrete reinforced with them has less permeability and capillary porosity, which prevents the pores in the concrete from becoming blocked. These gains are made possible by using the appropriate amount of polypropylene, which is 0.7 kg/m^3 (Kakooei, Akil, Jamshidi, & Rouhi, 2012; López-Buendía, Romero-Sánchez, Climent, & Guillem, 2013; Ramezanianpour, Esmaeili, Ghahari, & Najafi, 2013; Serrano, Cobo, Prieto, & de las Nieves González, 2016). The inclusion of polypropylene (PP) fibers in high and ultra-high-strength autoclaved mortars is a promising discovery that preserves practically all compressive strength properties without spalling up to 600°C temperature, even with a high silica fume concentration (Aydın, Yazıcı, & Baradan, 2008).

In addition, another study found that replacement of 10-30% of fine aggregate with crumb rubber reduced concrete unit weight and increased thermal and acoustic insulation (Sukontasukkul & Wiwatpattanapong, 2009). Furthermore, the inclusion of rubber increased the standard concrete's durability and deformation ability. Rubber crumbs have also been proven to successfully lower the danger of explosive spalling and the pace of concrete strength loss following exposure to high temperatures (Hernández-Olivares & Barluenga, 2004; Laperre et al., 2011). This is because rubber crumbs, when burned after being exposed to certain temperatures, can allow water vapor to escape from concrete, protecting the concrete skeleton from inflammable spalling. The continual water loss of the hydrated cement paste in the 105–850°C range and crystalline change from α-quartz to β-quartz in the 500–650°C range are both responsible for the rising strength degradation rate over 200°C (Bengar, Shahmansouri, Sabet, Kabirifar, & Tam, 2020).

In retrospect, there have been a few studies carried out with waste glass or waste ceramic incorporated with concrete, especially, in partial volumetric replacement of sand. There were separate studies with waste recycled glass or ceramics but no trace of a combined study. In this comprehensive study, variable amounts of crushed ceramic recycled aggregates (CRA) and crushed glass recycled aggregates (GRA) substituted with fine aggregates (sand) were employed to disclose the total residual structural strength of concrete in contrast to conventional normal concrete (NC) after preheating to various temperatures such as 100°C, 200°C, 400°C, 600°C, and 800°C. The Physico-chemical and mechanical behavior have been explored to divulge the thermal complexion of recycled concrete with waste glass and ceramic fines.

2. RESEARCH SIGNIFICANCE

Structural integrity and safety, serviceability, and design competency, regardless of structure type, have been a word of major importance in many scientific studies and technological developments across the world. Environmental exposure of glass and ceramic debris has been proved to be perilous. So, it calls for an attention to remove debris from the environment, more precisely, the use of CRA and GRA in concrete might be a useful research program since these materials possess enough structural strength to function as an electrical and thermal insulator during a fire. Because of the CRA and GRA's high melting point, greater durability and mechanical stability at elevated temperatures, such as 800°C, 900°C, or even more, it entails a larger region of interest and significance. The pre-firing and post-firing compressive strength of concrete blended with glass and ceramic fines replaced by sand must be determined, which is one of the core themes of this article. It also entails investigating the overall alterations in elastic modulus, tensile behaviors, and various mechanical properties of the heated candidate specimens made with different sand replacements. This study shows that glass recycled aggregate (GRA) and ceramic recycled aggregate (CRA) may be utilized as a fine aggregate substitute in concrete (up to 40%) for structural purposes. To the best of the authors' knowledge, this is the first combined study to look at the effect of altering the replacement amount of sand with recycled glass and ceramic fines with the goal of finding the top limit of its usefulness as a sustainable and lasting construction material without any prior treatment.

3. DETAILS OF THE EXPERIMENT

A. Materials and Mixtures

A pictorial representation of the constituent materials used in the study has been depicted in Figure 1.

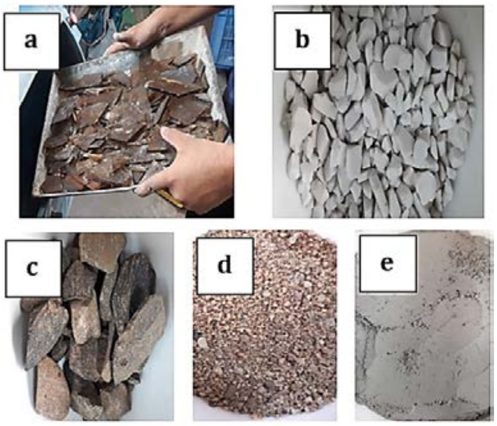

Figure 1: Types of aggregates (a) Crushed Glass (b) Crushed Ceramic (c) Coarse Aggregate (d) Fine Aggregate (e) Ordinary Portland Cement

i. Physical Properties of Aggregate

Several physical properties of natural coarse aggregate, natural fine aggregate, glass recycled aggregate, and ceramic recycled aggregate have been discussed in Table 1.

ii. Fine Aggregate (FA)

In this experiment, a locally available well-graded natural sand with a nominal maximum grain size of 4.75 mm was selected. ASTM C136-14 (A ASTM, 2014) is used for sand sieve analysis and gradation and a standard ASTM C29/29M-17a (17a, 2017) is used to determine the unit weight of FA. Furthermore, sand's specific gravity and water absorption capacity are determined using ASTM C128-15 (ASTM ASTM, 2015).

iii. Coarse Aggregate (CA)

The fraction of the naturally found stone coarse aggregates was kept within the range of 4.75-20mm whereas the maximum size was 19mm. The CA is sieved and graded according to ASTM C136-14 (A ASTM, 2014), while the unit weight is calculated using ASTM C29/29M-17a (17a, 2017). ASTM C127-15 (ASTM ASTM, 2015) is used to determine the CA's specific gravity and water absorption capacity.

Table 1
Physical Properties of aggregates

Variables	NCA	NFA	GRA	CRA
Apparent specific gravity	2.73	2.7	2.7	2.65
Bulk specific gravity (SSD)	2.71	2.6	2.6	2.45
Bulk specific gravity (OD)	2.7	2.46	2.46	2.34
Absorption capacity (%)	0.46	3.5	3	5
Fineness modulus	6.51	2.8	2.7	2.65
Loose unit weight (kg/m^3)	1477.02	1489	1489	1465
Compact unit weight (kg/m^3)	1525.57	1633	1633	1610
% of voids (Loose)	45.1	38.3	37.5	35.7
% of voids (Compact)	43.3	33	33.7	32.9
Abrasion value (%)	14.58	-	32	33.5

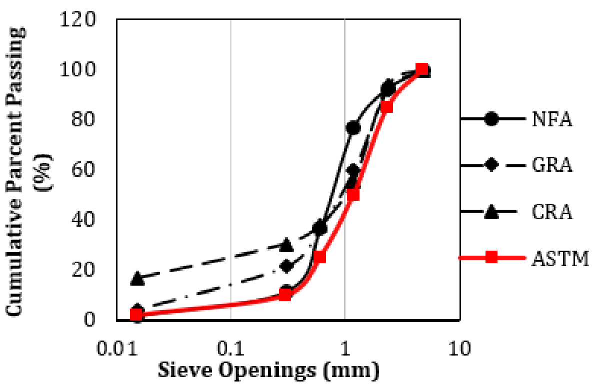

Figure 2: Particle size distribution of aggregates

In addition, the abrasion test is carried out in accordance with ASTM C131-14 (C131/131M, 2014). The particle size distribution of NCA, NFA, GRA, CRA, and ASTM standard is represented in Figure 2.

iv. Cement

As a binding material, Ordinary Portland Cement (OPC) of grade 52.5 was used to carry out the research. From Table 2, the setting time test of the cement paste was performed according to ASTM C191-18a (C191-18a, 2018). In order to govern the normal consistency of OPC cement, ASTM C187-16 (Standard, 2016) code was followed.

Table 2
Properties of Ordinary Portland Cement (52.5 grade)

Specific gravity (g/cm^3)	3.15
Initial setting time (min)	82
Final setting time (min)	229
Consistency (%)	31.5

v. Recycled Ceramic Fines (RCF)

When applied to concrete constructions as a partial replacement of sand, ceramics display enormous structural strength as well as suitable hardness. The waste ceramics were collected from the nearby ceramic factory and later, they were crushed via LA machine and also by manual hammer crushing. Sieve analysis of waste ceramics was conducted to discover the fineness modulus. With a density of 2-6 gms/cm^3, inorganic, metallic, or non-metallic crystalline ceramics with both ionic and covalent bonding have high melting points ranging from 1000°C-1600°C or even higher. The paper (Effting, Folgueras, Güths, & Alarcon, 2010) studied the chemical analysis of ceramics is discussed in Table 3.

Table 3
Chemical components of ceramic

Chemical components (%)	Ceramic powder (%)	Residue (%)
SiO_2	63.36	64.20
Al_2O_3	18.20	18.32
Fe_2O_3	2.77	0.65
CaO	1.74	1.09
Na_2O	0.34	1.95
K_2O	3.87	1.84
MnO	0.02	0.06
TiO_2	0.80	0.26
MgO	2.04	6.63
P_2O_5	0.05	0.06
PF	6.80	4.96

vi. Recycled Glass Fines (RGF)

Recycled glass as a partial substitute for fine aggregate (sand) has superior temperature resistance and melting point (1200-1600°C or more). The waste glass materials were collected from a local glass company to conduct the study. Employing an L.A. machine and manual mechanical hammer, waste glasses were crushed. Mechanical sieving was carried out to determine the fineness modulus and it was almost closer to sand's fineness modulus. The chemical composition of glass materials has been discussed in (M. Bignozzi, Saccani, Barbieri, & Lancellotti, 2015), especially those collected from different sources as depicted in Table 4.

B. Mix Proportions

Nine (09) different mixes of concrete cylinders were meant to be investigated at pre-firing and post-firing stages to reveal the physical and chemical alterations. Concrete mixes of different types have been displayed via specimen identification represented in Table 5 . Initially, M40 or 40 MPa target benchmark was set for determining the compressive strengths of the specimens after 28 days of curing episode at 19±2°C. After mechanical sieving, the fineness modulus of NCA (6.51), NFA (2.8), GRA (2.70), and CRA (2.65) were calculated. Throughout the entire study, the water-cement (w/c=0.42) ratio was kept constant and the density of Ordinary Portland Cement was observed 435kg/m^3 to maintain the uniformity in subsequent trials and tests. The term "uniformity" is mentioned to describe that, the volumetric alterations would occur in NFA, CRA, and GRA only while, there would be no change in cement, NCA, and water content.

Table 4
Chemical composition of glass

Chemical Components	Soda lime glass	Fluorescent lamps	Funnel glass	Crystal glass
SiO_2	70.40	68.47	56.11	58.64
Al_2O_3	2.06	2.26	3.02	0.02
TiO_2	<0.01[a]	<0.01[a]	0.08	<0.01[a]
Fe_2O_3	<0.01[a]	0.08	0.09	0.21
CaO	11.30	5.13	2.56	0.12
MgO	1.47	2.98	1.86	0.29
Sb_2O_3	<0.01[a]	0.08	0.17	0.22
ZnO	<0.01[a]	<0.01[a]	0.14	1.18
BaO	0.12	0.95	2.20	<0.01[a]
K_2O	1.21	1.61	10.01	7.21
Na_2O	13.4	17.65	5.46	4.67
PbO	<0.01[a]	0.79	18.34	27.43
Na_2Oeq[b]	13.90	18.55	12.97	8.95

[a] Data below the instrument detection limit
[b] Amount of (Na_2O+K_2O) expressed as soda equivalent content

Table 5
Identification of concrete specimens

Identification: $(GRA)_xF_z$ & $(CRA)_yF_z$	Description
NC	Normal concrete
GRA	Glass Recycled Aggregate
CRA	Ceramic Recycled Aggregate
F	Fine aggregate (sand)
x	% of GRA replacement against sand
y	% of CRA replacement against sand
z	% of existing fine aggregate (sand)

Table 6
Mix Ratio of ingredients for normal concrete
(per cubic meter of concrete)

Concrete strength (MPa)	NCA (Kg)	NFA (Kg)	Cement (Kg)	Water (Kg)	W/C Ratio
40	993.7	693.5	435	182.7	0.42

From the statistics expressed in Table 6, for 1m^3 of concrete, a combination of the unit contents of NCA, and NFA were measured successively 993.7kg and 695kg. Similarly, the quantities of cement and water were found consecutively 435kg and 182.5kg to design 1m^3 of concrete. Only NFA, GRA, and CRA were altered volumetrically in the subsequent trials.

Referring to Table 1, the bulk specific gravities of the materials were found somewhat different. In order to determine the mechanical properties of concrete with recycled ceramic and glass fines, volumetric partial alterations of natural sand (NFA) with GRA and CRA have been maintained. Volumetric partial replacements of NFA with GRA and CRA were kept 0%, 5%, 10%, 15%, 20%, 25%, 30%, 35%, and 40% throughout the study. In addition, Table 7 reveals the mix proportioning of various aggregates with respect to the concrete volume of $1m^3$. A 25°C temperature was taken into consideration as normal room temperature as the pre-firing stage and post-firing stages were 100°C, 200°C, 400°C, 600°C, and 800°C.

C. Concrete Specimens

To reveal the physical and chemical identities after 28 days of curing episode, a total of 306 cylinders were cast. Out of 306 cylinders, 18 cylinders were of conventional concrete while 288 cylinders were of CRA (144) and GRA (144) which are presented in Table 7. The dimensions of used molds were uniform in sizes of 100 mm by 200 mm.

Table 7

Aggregates' mix proportion per $1m^3$ of concrete volume

	Batch code	Proportions of fine aggregate (%)			NCA (kg/m³)	NFA (kg/m³)	Replaced NFA (kg/m³)	Cement (kg/m³)	Water (kg/m³)
		NFA	GRA	CRA					
1	$(GRA)_{0}F_{100}$	100	0	-	993.7	693.5	0	435	182.7
2	$(GRA)_{5}F_{95}$	95	5	-	993.7	658.83	34.67	435	182.7
3	$(GRA)_{10}F_{90}$	90	10	-	993.7	624.15	69.35	435	182.7
4	$(GRA)_{15}F_{85}$	85	15	-	993.7	589.48	104.02	435	182.7
5	$(GRA)_{20}F_{80}$	80	20	-	993.7	554.8	138.7	435	182.7
6	$(GRA)_{25}F_{75}$	75	25	-	993.7	520.13	173.37	435	182.7
7	$(GRA)_{30}F_{70}$	70	30	-	993.7	485.45	208.05	435	182.7
8	$(GRA)_{35}F_{65}$	65	35	-	993.7	450.78	242.72	435	182.7
9	$(GRA)_{40}F_{60}$	60	40	-	993.7	416.1	277.4	435	182.7
10	$(CRA)_{5}F_{95}$	95	-	5	993.7	660.25	34.75	435	182.7
11	$(CRA)_{10}F_{90}$	90	-	10	993.7	625.5	69.5	435	182.7
12	$(CRA)_{15}F_{85}$	85	-	15	993.7	590.75	104.25	435	182.7
13	$(CRA)_{20}F_{80}$	80	-	20	993.7	556	139	435	182.7
14	$(CRA)_{25}F_{75}$	75	-	25	993.7	521.25	173.75	435	182.7
15	$(CRA)_{30}F_{70}$	70	-	30	993.7	486.5	208.5	435	182.7
16	$(CRA)_{35}F_{65}$	65	-	35	993.7	451.75	243.25	435	182.7
17	$(CRA)_{40}F_{60}$	60	-	40	993.7	417	278	435	182.7

Table 8

Mix proportioning of concrete cylinders at elevated temperatures

Temperatures	25°C	100°C	200°C	400°C	600°C	800°C	
% Replacement							Total
0	3	3	3	3	3	3	18
	GRA+CRA						
5	3+3	3+3	3+3	3+3	3+3	3+3	36
10	3+3	3+3	3+3	3+3	3+3	3+3	36
15	3+3	3+3	3+3	3+3	3+3	3+3	36
20	3+3	3+3	3+3	3+3	3+3	3+3	36
25	3+3	3+3	3+3	3+3	3+3	3+3	36
30	3+3	3+3	3+3	3+3	3+3	3+3	36
35	3+3	3+3	3+3	3+3	3+3	3+3	36
40	3+3	3+3	3+3	3+3	3+3	3+3	36
						Total cylinders	**306**

D. Experimental Program

After the initial mix design, associated materials were collected whereas waste glasses and ceramics were crushed in a Los Angeles (L.A.) machine to bring the crushed materials into as finer forms as natural sand. Sieve analyses of NCA, NFA, GRA, and CRA were then carried out and materials were arranged as per the replacement ratio of recycled glass and ceramic fines against natural sand using a weighing scale. The final mixing of the materials was accumulated into a mechanical mixer machine maintaining an appropriate w/c ratio (0.42). After each mix, the slump value of newly prepared concrete was measured according to ASTM C143-15(Standard, 2015). The specimens were first cured in a damp environment for 24 hours before being demolded and stored in a continuous state under fresh water at a regulated laboratory temperature of 19±2°C before being tested. ASTM C39-18(C39, 2018) is used to perform the 28-days compressive strength test. The splitting tensile strength of the concrete cylinders was also investigated after 28 days in accordance with ASTM C496-17(Concrete & Aggregates, 2017). Initially, at the pre-firing stage, the compressive strength of 51 cylinders where 3 of normal concrete (0% sand replacement) and 24 cylinders from both GRA and CRA was calculated at room temperature of 25°. A conventional gas furnace was used in this study to facilitate the firing episode of normal concrete cylinders. The time duration of each heating stage was 1 hour for 100°C, 200°C, 400°C, 600°C, and 800°C at an average rate of 8-9°C/min. There were 3 normal concrete cylinders in every heating temperature, while 24 cylinders from both batches of GRA and CRA. Concrete specimens were then cooled down at room temperature and then the specimens were taken to measure compressive strength.

4. RESULTS AND DISCUSSION

A. Monitoring of Change in the Microstructures at Elevated Temperature

By opening the door when the interior temperature of the conventional gas furnace reached the desired temperature, the circumstances that happened during the heating process were seen and recorded in a data-logger connected laptop associated with 3 thermocouples.

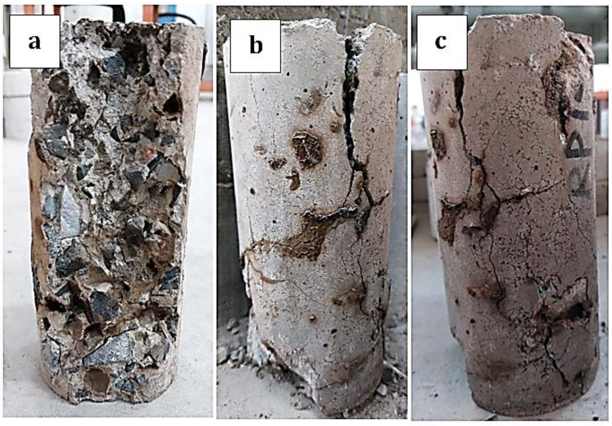

Figure 3: Concrete failures at 800°C (a) NC, (b) GRA (35%), and (c) CRA (35%)

Hardened concrete expands when the temperature increases and finally shrinks due to the loss of water as a form of water vapor. Pictorial illustration from Figure 3 specified the explosive spalling with several larger cracks that appeared on the surface of the concrete when it was 800°C.

i. Analysis of Change in the Microstructure of Normal Concrete

Up to 100°C, no significant alterations except water vapor in normal concrete were detected. When it is recorded at 200°C, some negligible micro-cracks, which were hardly visible were observed and slightly different than the observations made in the literatures (X. Li, Li, Onofrei, Ballivy, & Khayat, 1999; Lin, Lin, & Powers-Couche, 1996). At 400°C, micro-cracks began to expose their intensity evenly over the concrete surface which has been also found similar in previous studies (Arioz, 2007; Aydın & Baradan, 2007; Biolzi, Cattaneo, & Rosati, 2008; Handoo, Agarwal, & Agarwal, 2002; Hossain, 2006; Lau & Anson, 2006; Matesová, Bonen, & Shah, 2006; Peng, Chan, Yan, Liu, & Yi, 2005; Wang, Wu, & Wang, 2005). Comparatively larger cracks (1.5-3.5mm) were visible when the temperature reached 600°C. At temperatures exceeding 600°C, certain minerals in rocks, such as quartz, dissolve or transform. This occurs because concrete undergoes an allotropic transition with a large volume change at 573°C(Zega & Di Maio, 2009, Mujib *et al.*, 2022). At 800°C, explosive cracking with concrete spalling at the edges was observed in conventional concrete which is displayed in Figure 3(a). Thermal expansion, concrete shrinkage while drying, and water evaporation at high temperatures all contributed to cracking(Son, Hajirasouliha, & Pilakoutas, 2011).

ii. Analysis of Change in the Microstructure of GRA Concrete

No significant effect due to temperature increment in GRA_{35} concretes was noticed up to 400°C. Micro-cracks that appeared in GRA_{35} concrete after heating to 400°C were less intense than normal conventional concrete. Fewer cracks occur in GRA_{35} concrete since glass possesses impermeability, superior flow nature, and higher strength exposure to elevated temperatures which is also supported by the previous study (Terro, 2006). Cracks become significant over the surface of GRA_{35} concrete with some minor spalling when heated up to 600°C. Explosive cracking appeared with less concrete spalling than normal concrete along the edges when GRA_{35} experienced heating up to 800°C. This happened since glass normally melts at temperature not less than 700°C, when heated up to 800°C, slowly glass fines turn into a state of liquid and re-solidified when concrete is cooled down (M.-Z. Guo, Chen, Ling, & Poon, 2015).

iii. Analysis of Change in the Microstructure of CRA Concrete

Fewer cracks and spalling were noticed in CRA_{35} than in NC and GRA_{35} when the temperature was in the range of 25°C to 600°C. The visual observation of the appeared results pointed out that explosive patterns and micro-cracks were more significant in GRA than CRA concrete even after heating episodes up to 800°C. After heating to 800°C, less spalling along the edges of the cylinder of CRA was noticed but it was slightly more in GRA concrete. This is due to the higher melting point of ceramic, and better internal cohesiveness of ceramic fines with concrete mortar, which in return helped CRA concrete retain the bond in concrete enduring higher temperatures.

In addition, as temperature increases, more abrupt alterations and failures are found in NC relative to the recycled concretes. Furthermore, superiority over NC was found due to the better internal cohesion among the particles, rough geometric surfaces of crushed glass and ceramic fines, and superior physical and chemical properties of glass and ceramic particles

B. Observation of Concrete Rheology and Consistency

The rheological identity of fresh concrete is determined by the consistency parameter, precisely the conventional slump test, which is illustrated in the Figure 4**.** In comparison to the other 16 concrete mixtures, the normal concrete has a greater slump value of 112 mm. This suggests that the combination of normal concrete is the most workable for the specimens under investigation. Initially, up to 15% replacement in both GRA and CRA, it distinctly provides the slightly higher workability of concrete made with GRA than CRA. When the replacement is 5% in both concrete mixes, GRA_5 concrete is found to be 3.85% higher than CRA_5 concrete. With the increasing replacement trend in concrete mixes, GRA_{15} is noticed 0.97% greater than CRA_{15}. Up to 15% sand replacement in concrete, the graphical illustration depicts the comparatively higher water demand propensity in GRA than CRA concrete due to the greater surface area of glass fines. It clearly indicates that the consistency of both recycled concretes is declining with incrementing replacement rate.

Due to the non-uniform texture, higher particle roughness, and angular shape of the glass and ceramic fines compared to natural fine sand, the inclusion of glass or ceramic fines reduces the workability of concrete. A similar result was obtained in the previous study (Ismail & Al-Hashmi, 2008). However, a higher slump value is observed in the successive mixes of CRA_{20} to CRA_{40}. For CRA_{40}, the slump value is recorded 101 mm which is 3.06% higher than GRA_{40}. More inclusion of recycled ceramic and glass fines as partial replacement of sand creates greater interlocking in concrete due to higher absorption rate and roughness of the surface.

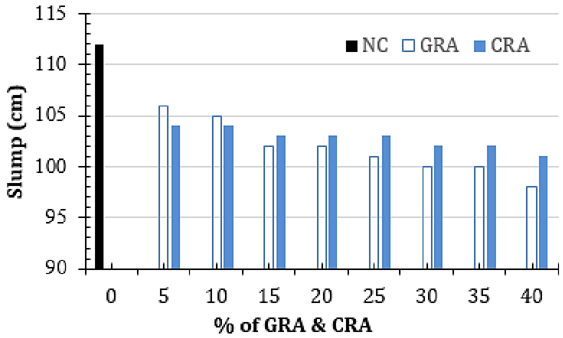

Figure 4: Slump value of varying concrete mixtures

The slump value of normal concrete mix is 112 mm, while the mean slump value for all the mix proportions was observed at approximately 102.60 mm for GRA and 102.75 mm for CRA.

C. Compressive Strength

The compressive strength of concrete samples, after a curing episode of 28 days, changed instantly after a 1-hour heating interval. Evaluation of fire resistivity of recycled concrete with crushed glass and ceramic fines relative to normal concrete is delineated in Figure 5 and Figure 6. At 25°C, the compressive strength of NC is seen 33.86 MPa, however, for CRA_5, CRA_{30}, and CRA_{40}, the readings showed successively 34.4 MPa (1.6% increment), 43.16 MPa (27.47% increment), and 50 MPa (47.67% increment) in comparison with NC. Simultaneously, the strength readings of GRA_5, GRA_{30}, and GRA_{40} at 25°C were consecutively 32.8 MPa (3.23% reduction), and 45.64 MPa (34.79% increment), and 47.18 MPa (39.34% increment) relative to NC. The highest replacements in concrete combinations, such as CRA_{40} and GRA_{40}, also observe the extreme decline of strengths along with concrete spalling as the heating episode lasts for 1 hour. The graphical trend illustrates that the strength reduction is 55.11% for NC when the temperature jumps up from 25°C to 600°C, while it is recorded 49.08% for CRA_{30} and 44.98% for GRA_{30} in a similar fashion.

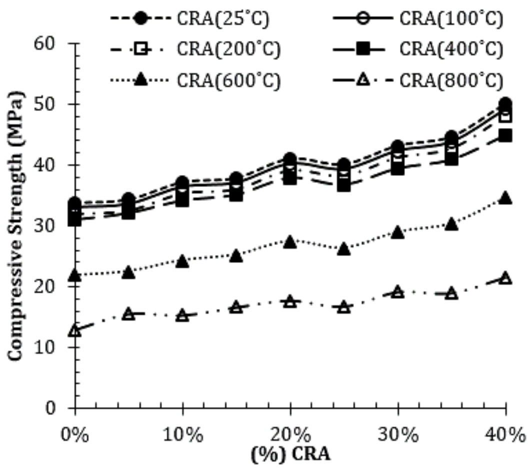

Figure 5: Compressive strength at different temperatures (CRA)

The function of compressive strength of recycled concretes demonstrates that with the increasing replacement of sand with CRA and GRA, strength increases positively. Due to the irregular geometric shape of crushed glass and ceramic, smooth interlocking and inter-particle cohesiveness in concrete mortar escalate (Özkan & Yüksel, 2008; Westerholm, Lagerblad, Silfwerbrand, & Forssberg, 2008, Mujib *et al.*, 2022). At 800°C, the compressive strength of NC is observed 12.93 MPa, while it is 19.11 MPa and 19.82 MPa consecutively for CRA_{30} (47.80% increment) and GRA_{30} (53.28% increment). The highest level of sand replacement (40%) in CRA concrete provides better strength than GRA concrete at 800°C. The increase in strength for CRA_{40} concrete is 66.20% greater than NC but for GRA_{40}, it is 61.41% greater than NC.

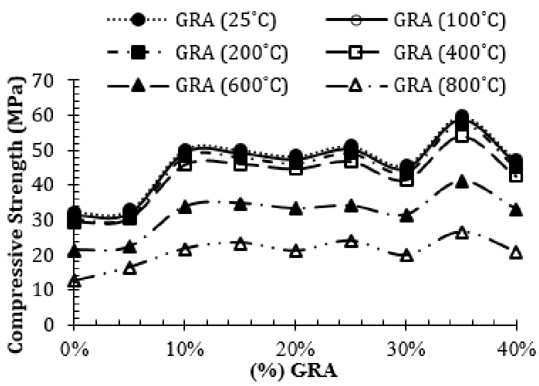

Figure 6: Compressive strength at different temperatures (GRA)

D. Splitting Tensile Strength

In accordance with ACI 318-14(ACI, 2014), the findings of splitting tensile strengths at 28 days for various concrete mixtures are displayed in Figure 7. According to ACI 318-14 the equation of mean splitting tensile strength is provided below.

$$f_{ctm,sp} = 0.556\sqrt{f'_c} \quad (1)$$

where f'_c is compressive strength in MPa and $f_{ctm,sp}$ is mean splitting tensile strength in MPa.

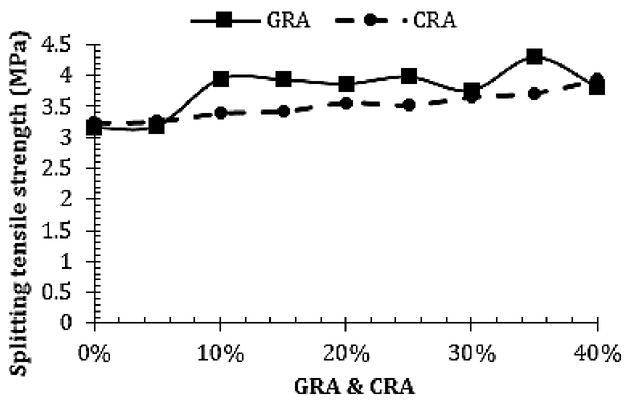

Figure 7: Splitting tensile strength of GRA and CRA concrete

It has been observed that at room temperature (25°C), normal concretes' splitting tensile strength was found 3.15 MPa, while it is noticed 3.18 MPa for GRA_5 and 3.26 MPa for CRA_5 with an increment of successively 0.95% and 3.49% in comparison with normal concrete. The trend depicts that the splitting tensile strength of GRA is consistently higher than CRA. The least difference in strength is noticed when the replacement is 30% for both. The greatest increment is noticed for GRA_{35} and it is 4.21 MPa with a raise of 36.19% against NC. In addition, when the replacement is increased to 40% for both GRA and CRA, the highest increase is seen in CRA_{40} with a 24.76% while it is 20.95% for GRA_{40}.

Despite the abrupt changes, the splitting tensile strength of concrete increases as the amount of recycled glass and recycled ceramic in the concrete mixture increase due to its high tensile capacity. This might be due to the existence of recycled glass and ceramic fines along the fracture plane before it splits, which provides a strong profile of the aggregate-cement paste link.

E. Variations in Poisson's Ratio

While investigating the mechanical properties of recycled concretes along with normal concrete, which is presented in Table 9, average Poisson's ratios of candidate concrete cylinders have been observed. There is an increment of 4.74% in Poisson's ratio in GRA_5 and 11.86% in CRA_5 were found compared to the Poisson's ratio of 0.253 for NC. It defines the soft and smooth nature of recycled glass and ceramic fines with a superior quality of energy absorption to normal concrete. Furthermore, when the maximum volumetric replacement (40%) was taken into consideration, the Poisson's ratio of CRA_{40} exhibited a 47.16% increment compared to the Poisson's ratio of GRA_{40} (0.229). Ceramic fines effectively exhibited cracking by forming a strong, internal aggregate-mortar link, which keeps the aggregate particles together and provides less cracking than glass fines.

Table 9
Mechanical properties of different recycled concrete mixtures at 28 days

Batch ID	Peak stress (MPa)	Axial strain at peak stress	Transverse strain at peak stress	Ultimate strain	Poisson's ratio
NC	33.86	0.00265	0.000671	0.00311	0.253
$(GRA)_5F_{95}$	32.8	0.00391	0.00104	0.00391	0.265
$(GRA)_{10}F_{90}$	50.25	0.00201	0.000612	0.00273	0.304
$(GRA)_{15}F_{85}$	50.06	0.00227	0.000593	0.00281	0.261
$(GRA)_{20}F_{80}$	48.29	0.00243	0.000582	0.00271	0.239
$(GRA)_{25}F_{75}$	51.24	0.00245	0.000592	0.00262	0.242
$(GRA)_{30}F_{70}$	45.64	0.00239	0.000508	0.0021	0.213
$(GRA)_{35}F_{65}$	59.72	0.00205	0.000738	0.000282	0.360
$(GRA)_{40}F_{60}$	47.18	0.00253	0.000579	0.00278	0.229
$(CRA)_5F_{95}$	34.4	0.00288	0.000814	0.00276	0.283
$(CRA)_{10}F_{90}$	37.21	0.00276	0.000805	0.00271	0.292
$(CRA)_{15}F_{85}$	37.92	0.00266	0.000801	0.00279	0.301
$(CRA)_{20}F_{80}$	41.03	0.00259	0.000795	0.00275	0.301
$(CRA)_{25}F_{75}$	40.16	0.0026	0.000798	0.00277	0.307
$(CRA)_{30}F_{70}$	43.16	0.00253	0.000783	0.00267	0.309
$(CRA)_{35}F_{65}$	44.66	0.00248	0.000771	0.00279	0..311
$(CRA)_{40}F_{60}$	50	0.00227	0.000765	0.00286	0.337

F. Modulus of Elasticity

For a better understanding of the mechanical properties of recycled concrete, a clear overview of modulus of elasticity is required to discussed accordingly. From the trend derived from Figure 8, it is visible that with the increase in recycled ceramic and glass fines in concrete mixes, the modulus of elasticity increases in comparison with normal concrete.

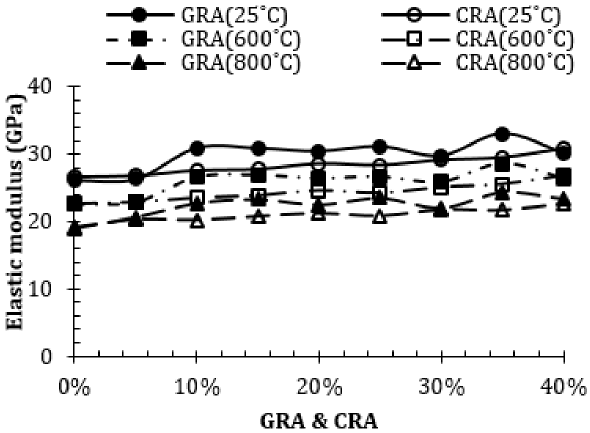

Figure 8. Modulus of elasticity of GRA and CRA concrete

At 25°C, the elastic modulus of 26.61 GPa is achieved for NC, while in CRA (20%) it is (28.59 GPa) which is 7.44% greater than NC but in the case of GRA, it is 14.32% greater than NC. At 600°C, the elastic modulus is 22.58 GPa for NC while the increment is observed 25.85% and 12.39% successively for GRA_{35} and CRA_{35}. For CRA_{40}, the elastic modulus is 18.31% greater than NC whereas it is 22.38% greater than NC for GRA. The study reveals that the quantitative alterations are simpler and slower in CRA than in GRA with increasing temperatures. Furthermore, the modulus of elasticity data specified the fact, more precisely, that CRA and GRA in concrete mixes make the concrete more stable and less fragile in tension than normal concrete.

G. Predicted Equation for Compressive and Tensile Strength

The mathematical equations for predicting the compressive strength of CRA and GRA were formulated by following the regression analysis. This operation which was performed by statistical analysis software (SPSS), resulted in a multiple linear regression model presented in Equations (2) and (3). The data for compressive strength presented in Figure 5 and Figure 6 were used during the analysis. These equations can predict for CRA/GRA substitution ratio of 0–60% accurately. Two variables, “t” temperature of the concrete and “r” CRA/GRA replacement ratio, were included as independent variables while the compressive (f'_c) strength as the dependent variable. The SPSS output results indicate that the adjusted R-square values were 86% and 97%, respectively for CRA and GRA compressive strength equations. The statistical test for the two models was proven to be significant as the p-values associated with the F-test and the t-test were less than 0.001. The validation results of equations (2) and (3) are presented in Figure 9a and 9b, and as seen, the models are predicting the strength for CRA and GRA (for all mixtures) with reasonable accuracy.

$$f_c'(CRA) = 31.72 + 131.96r - 0.021tr - 4.37e^{-8}t^3 - 224.55r^2 \quad (2)$$

$$f_c'(GRA) = 32.7 + 35.28r + 1.69e^{-13}t^5 - 1.83e^{-10}t^4 - 2.41e^{-5}t^2 \quad (3)$$

where, f'_c = compressive strength (MPa), t = temperature, and r = CRA/GRA substitution ratio (fractions).

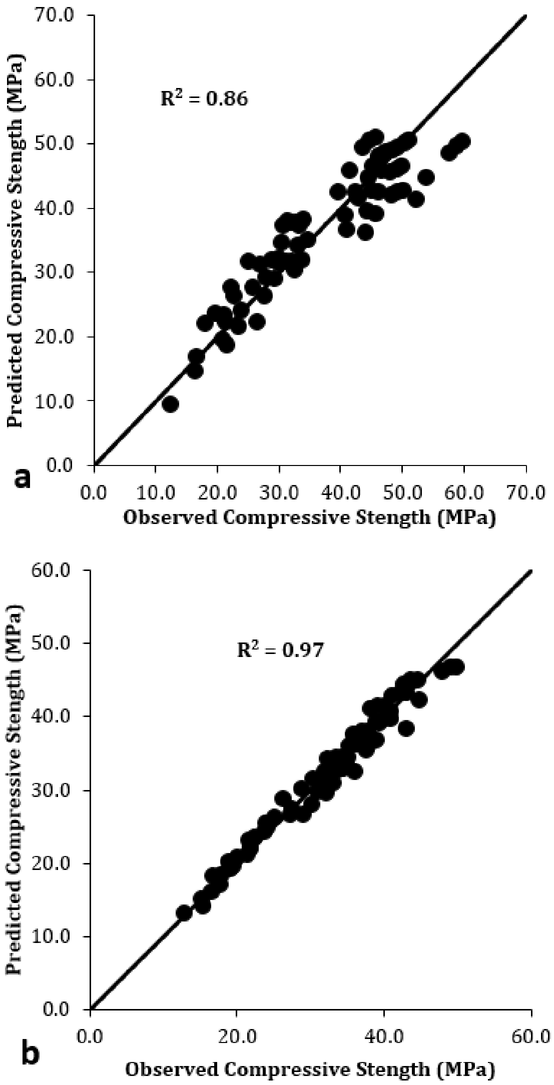

Figure 9: Comparison between the predicted and observed compressive strength values: a) CRA; b) GRA

5. CONCLUSION

The mechanical properties of recycled concrete with crushed glass and ceramic fines as partial substitutions of natural sand are extensively explored in this work. Following is a synopsis of the study's findings:

- Strength is observed to be raised with the increasing replacement of both crushed ceramic and glass particles in a comprehensive investigation of statistical values of compressive strengths. Though it is noticed that 3.13% strength reduction occurs for GRA_5 at 25°C, all other values were almost consistent. This may be due to the mechanical reading error or improper curing on that particular cylinder. The maximum strength is found for GRA_{35} (59.72 MPa), while it is 50 MPa for CRA_{40} at 25°C. From 25°C to

800°C, the strength reduction rate is somewhat more in CRA_{40} (57.02%) compared to GRA_{40} (55.77%).

- Slump value falls when the amount of fine sand substitutions (crushed ceramic and glass fines) in concrete mixes increases. Since glass and ceramic fines exhibit non-uniformity, higher angularity, and superior roughness compared to natural sand, workability reduces in recycled concretes.
- The increasing rate of involvement of recycled glass and ceramic fines create comparatively stronger bonds along the fracture plane than normal concrete, hence more durable in nature. Splitting tensile strength of NC at 25°C is 3.15 MPa, however, 0.95% and 3.49% increment is found consecutively for GRA_5 and CRA_5. With a 24.76% increase, CRA_{40} has the biggest increase, while GRA_{40} has a 20.95% gain relative to NC.
- The concrete made with recycled glass and ceramic fines exhibited a smoother nature with an intensified capacity of energy assimilation compared to normal concrete. With the increasing proportions of recycled glass and ceramic fines, Poisson's ratio has been observed to be increasing compared to normal concrete. Maximum percent increment was obtained in the Poisson's ratio of CRA_{40} (47.16%) when compared to the Poisson's ratio of GRA_{40} (0.229).
- Comprehensive analysis of the study discloses that among the concrete mixes, CRA_{35}, $CRA_{40,}$ and GRA_{35}, GRA_{40} exhibit better performance against at elevated temperatures. The trend derived from the modulus of elasticity also reveals that it is 18.31% higher in CRA_{40} than in NC, although it is 22.38% higher in GRA_{40}. Hence, the recycled concretes with the highest inclusion of glass and ceramic fines are less fragile in tension than normal concrete.

Sustainable development along with green technology is the core essence of civil engineering construction. It can be achieved by exploiting the waste materials such as ceramic and glass in concrete, which are among the potential sources of landfills. In addition, due to the dredging activity of sand from river beds, banks of rivers erode. Furthermore, erosion will result in the loss of protection and shade from the bank vegetation. Efficient utilization of recycled materials (ceramic and glass) as substitutions for natural sand would help minimize the demand for sand to an extent, thus reducing the dredging activities of sand from the sea beds or river beds. The future investigation could incorporate the extensive replacement of sand by volume instead of the replacements used in this study to further investigate the effectiveness of fire responses along with other mechanical properties.

ACKNOWLEDGEMENTS

The authors would like to express his gratitude to the Department of Civil Engineering, Military Institute of Science and Technology, Dhaka, Bangladesh, and the Department of Civil Engineering, University of Alberta, Canada. They also would like to thank the Editors and anonymous reviewers of the article for their insightful suggestions and comments to improve the content.

REFERENCES

17a, A. C. M. (2017). Standard Test Method for Bulk Density ("Unit Weight") and Voids in Aggregate *ASTM International*. West Conshohocken, PA.

38, f. B. N. (2007). Fire Design of Concrete Structures - Materials, Structures and Modelling. Retrieved from https://www.fib-international.org/publications/fib-bulletins/fire-design-of-concrete-structures-pdf-detail.html

ACI. (2014). ACI 318-14. Building code requirements for structural concrete: ACI Farmington Hills, MI, USA.

Adaway, M., & Wang, Y. (2015). Recycled glass as a partial replacement for fine aggregate in structural concrete–Effects on compressive strength. *Electronic Journal of Structural Engineering, 14*(1), 116-122.

Al-Sibahy, A., & Edwards, R. (2012). Mechanical and thermal properties of novel lightweight concrete mixtures containing recycled glass and metakaolin. *Construction and Building Materials, 31*, 157-167.

Al Bakri, A., Norazian, M., Kamarudin, H., Salleh, M., Anuar, M. A., & Alida, A. (2013). *Strength of concrete based cement using recycle ceramic waste as aggregate.* Paper presented at the Advanced materials research.

Ali, F., Nadjai, A., Silcock, G., & Abu-Tair, A. (2004). Outcomes of a major research on fire resistance of concrete columns. *Fire Safety Journal, 39*(6), 433-445. doi:https://doi.org/10.1016/j.firesaf.2004.02.004

Arioz, O. (2007). Effects of elevated temperatures on properties of concrete. *Fire safety journal, 42*(8), 516-522.

ASTM, A. (2014). C136/C136M–14. *Standard Test Method for Sieve Analysis of Fine and Coarse Aggregates, ASTM International, West Conshohocken, PA.*

ASTM, A. (2015). Standard test method for relative density (specific gravity) and absorption of coarse aggregate. *ASTM West Conshohocken, PA.*

Aydın, S., & Baradan, B. (2007). Effect of pumice and fly ash incorporation on high temperature resistance of cement based mortars. *Cement and concrete research, 37*(6), 988-995.

Aydın, S., Yazıcı, H., & Baradan, B. (2008). High temperature resistance of normal strength and autoclaved high strength mortars incorporated polypropylene and steel fibers. *Construction and Building Materials, 22*(4), 504-512. doi:https://doi.org/10.1016/j.conbuildmat.2006.11.003

Bednář, J., Wald, F., Vodička, J., & Kohoutková, A. (2013). Experiments on membrane action of composite floors with steel fibre reinforced concrete slab exposed to fire. *Fire Safety Journal, 59*, 111-121.

Bengar, H. A., Shahmansouri, A. A., Sabet, N. A. Z., Kabirifar, K., & Tam, V. W. (2020). Impact of elevated temperatures on the structural performance of recycled rubber concrete: Experimental and mathematical modeling. *Construction and Building Materials, 255*, 119374.

Bignozzi, M., Saccani, A., Barbieri, L., & Lancellotti, I. (2015). Glass waste as supplementary cementing materials: The effects of glass chemical composition. *Cement and Concrete composites, 55*, 45-52.

Bignozzi, M. C., & Saccani, A. (2012). Ceramic waste as aggregate and supplementary cementing material: A combined action to contrast alkali silica reaction (ASR). *Cement and Concrete composites, 34*(10), 1141-1148.

Biolzi, L., Cattaneo, S., & Rosati, G. (2008). Evaluating residual properties of thermally damaged concrete. *Cement and Concrete Composites, 30*(10), 907-916.

C39, A. (2018). Standard Test Method for Compressive Strength of Cylindrical Concrete Specimens. West Conshohocken, PA: ASTM International.

C131/131M, A. (2014). Standard Test Method for Resistance to Degradation of Small-Size Coarse Aggregate by Abrasion and Impact in the Los Angeles Machine. West Conshohocken, PA,: ASTM International.

C191-18a, A. (2018). Standard Test Methods for Time of Setting of Hydraulic Cement by Vicat Needle. West Conshohocken, PA: ASTM International.

Chen, S.-H., Chang, C.-S., Wang, H.-Y., & Huang, W.-L. (2011). Mixture design of high performance recycled liquid crystal glasses concrete (HPGC). *Construction and Building Materials, 25*(10), 3886-3892.

Colombo, M., & Felicetti, R. (2007). New NDT techniques for the assessment of fire-damaged concrete structures. *Fire Safety Journal, 42*(6-7), 461-472.

Concrete, A. I. C. C. o., & Aggregates, C. (2017). *Standard test method for splitting tensile strength of cylindrical concrete specimens1*: ASTM international.

Corinaldesi, V., Gnappi, G., Moriconi, G., & Montenero, A. (2005). Reuse of ground waste glass as aggregate for mortars. *Waste Management, 25*(2), 197-201.

de Brito, J., Pereira, A., & Correia, J. (2005). Mechanical behaviour of non-structural concrete made with recycled ceramic aggregates. *Cement and Concrete composites, 27*(4), 429-433.

de Castro, S., & de Brito, J. (2013). Evaluation of the durability of concrete made with crushed glass aggregates. *Journal of Cleaner Production, 41*, 7-14.

Dilek, U. (2005). Evaluation of fire damage to a precast concrete structure nondestructive, laboratory, and load testing. *Journal of performance of constructed facilities, 19*(1), 42-48.

Dong, H., Cao, W., Bian, J., & Zhang, J. J. M. (2014). The fire resistance performance of recycled aggregate concrete columns with different concrete compressive strengths. *7*(12), 7843-7860.

Dos Santos, J., Branco, F. A., & de Brito, J. (2002). Assessment of concrete structures subjected to fire—the FBTest. *Magazine of concrete Research, 54*(3), 203-208.

Effting, C., Folgueras, M. V., Güths, S., & Alarcon, O. E. J. M. R. (2010). Microstructural characterization of ceramic floor tiles with the incorporation of wastes from ceramic tile industries. *13*(3), 319-323.

El-Dieb, A. S., Taha, M. R., & Abu-Eishah, S. I. (2019). The use of ceramic waste powder (CWP) in making eco-friendly concretes. *Ceramic Materials: Synthesis, Characterization, Applications and Recycling*, 1-35.

Federico, L., & Chidiac, S. (2009). Waste glass as a supplementary cementitious material in concrete–critical review of treatment methods. *Cement and Concrete composites, 31*(8), 606-610.

Fernández-Jiménez, A., Pastor, J. Y., Martín, A., & Palomo, A. J. J. o. t. A. C. S. (2010). High-Temperature Resistance in Alkali-Activated Cement. *93*(10), 3411-3417.

Fike, R., & Kodur, V. (2011). Enhancing the fire resistance of composite floor assemblies through the use of steel fiber reinforced concrete. *Engineering Structures, 33*(10), 2870-2878.

Georgali, B., & Tsakiridis, P. (2005). Microstructure of fire-damaged concrete. A case study. *Cement and Concrete composites, 27*(2), 255-259.

Guo, M.-Z., Chen, Z., Ling, T.-C., & Poon, C. S. (2015). Effects of recycled glass on properties of architectural mortar before and after exposure to elevated temperatures. *Journal of cleaner production, 101*, 158-164.

Guo, Y.-c., Zhang, J.-h., Chen, G.-m., & Xie, Z.-h. J. J. o. c. p. (2014). Compressive behaviour of concrete structures incorporating recycled concrete aggregates, rubber crumb and reinforced with steel fibre, subjected to elevated temperatures. *72*, 193-203.

Hager, I. (2013). Behaviour of cement concrete at high temperature. *Bulletin of the Polish Academy of Sciences. Technical Sciences, 61*(1), 145-154.

Halicka, A., Ogrodnik, P., & Zegardlo, B. (2013). Using ceramic sanitary ware waste as concrete aggregate. *Construction and Building Materials, 48*, 295-305. doi:https://doi.org/10.1016/j.conbuildmat.2013.06.063

Handoo, S., Agarwal, S., & Agarwal, S. (2002). Physicochemical, mineralogical, and morphological characteristics of concrete exposed to elevated temperatures. *Cement and concrete research, 32*(7), 1009-1018.

Heikal, M. (2000). Effect of temperature on the physico-mechanical and mineralogical properties of Homra pozzolanic cement pastes. *Cement and Concrete Research, 30*(11), 1835-1839.

Hernández-Olivares, F., & Barluenga, G. (2004). Fire performance of recycled rubber-filled high-strength concrete. *Cement and Concrete Research, 34*(1), 109-117.

Higashiyama, H., Sappakittipakorn, M., Mizukoshi, M., & Takahashi, O. (2014). Efficiency of ground granulated blast-furnace slag replacement in ceramic waste aggregate mortar. *Cement and Concrete composites, 49*, 43-49. doi:https://doi.org/10.1016/j.cemconcomp.2013.12.014

Higashiyama, H., Yamauchi, K., Sappakittipakorn, M., Sano, M., & Takahashi, O. (2013). A visual investigation on chloride ingress into ceramic waste aggregate mortars having different water to cement ratios. *Construction and Building Materials, 40*, 1021-1028.

Holan, J., Novak, J., Müller, P., & Štefan, R. (2020). Experimental investigation of the compressive strength of normal-strength air-entrained concrete at high temperatures. *Construction and Building Materials, 248*, 118662.

Hossain, K. M. A. (2006). High strength blended cement concrete incorporating volcanic ash: Performance at high temperatures. *Cement and Concrete Composites, 28*(6), 535-545.

Huseien, G. F., Sam, A. R. M., Mirza, J., Tahir, M. M., Asaad, M. A., Ismail, M., . . . Materials, B. (2018). Waste ceramic powder incorporated alkali activated mortars exposed to elevated Temperatures: Performance evaluation. *187*, 307-317.

Ismail, Z. Z., & Al-Hashmi, E. A. (2008). Use of waste plastic in concrete mixture as aggregate replacement. *Waste management, 28*(11), 2041-2047.

Jin, W., Meyer, C., & Baxter, S. (2000). " Glascrete"-Concrete with Glass Aggregate. *ACI Materials Journal, 97*(2), 208-213.

Kakooei, S., Akil, H. M., Jamshidi, M., & Rouhi, J. (2012). The effects of polypropylene fibers on the properties of reinforced concrete structures. *Construction and Building Materials, 27*(1), 73-77.

Khoury, G. (1992). Compressive strength of concrete at high temperatures: a reassessment. *Magazine of concrete Research, 44*(161), 291-309.

Khoury, G. A., Grainger, B. N., & Sullivan, P. J. (1986). Strain of concrete during first cooling from 600 C under load. *Magazine of concrete Research, 38*(134), 3-12.

Khoury, G. A. J. P. i. s. e., & materials. (2000). Effect of fire on concrete and concrete structures. *2*(4), 429-447.

Kim, J., & Lee, G.-P. (2015). Evaluation of mechanical properties of steel-fibre-reinforced concrete exposed to high temperatures by double-punch test. *Construction and Building Materials, 79*, 182-191.

Kong, D. L., Sanjayan, J. G., & Sagoe-Crentsil, K. (2007). Comparative performance of geopolymers made with metakaolin and fly ash after exposure to elevated temperatures. *Cement and Concrete Research, 37*(12), 1583-1589.

Kong, D. L. Y., Sanjayan, J. G., & Sagoe-Crentsil, K. (2005). *Damage due to elevated temperatures in metakaolinite-based geopolymer pastes.* Paper presented at the International Workshop on Geopolymer Cement and Concrete.

Lankard, D. R., Birkimer, D. L., Fondriest, F. F., & Snyder, M. J. (1971). Effects of moisture content on the structural properties of portland cement concrete exposed to temperatures up to 500F. *Special Publication, 25*, 59-102.

Laperre, K., Depypere, M., van Gastel, N., Torrekens, S., Moermans, K., Bogaerts, R., . . . Carmeliet, G. (2011). Development of micro-CT protocols for in vivo follow-up of mouse bone architecture without major radiation side effects. *Bone, 49*(4), 613-622.

Lau, A., & Anson, M. (2006). Effect of high temperatures on high performance steel fibre reinforced concrete. *Cement and concrete research, 36*(9), 1698-1707.

Lee, J., Choi, K., Hong, K. J. J. o. A. A., & Engineering, B. (2009). Color and material property changes in concrete exposed to high temperatures. *8*(1), 175-782.

Li, L.-J., Xie, W.-F., Liu, F., Guo, Y.-C., & Deng, J. (2011). Fire performance of high-strength concrete reinforced with recycled rubber particles. *Magazine of concrete Research, 63*(3), 187-195.

Li, M., Qian, C., & Sun, W. (2004). Mechanical properties of high-strength concrete after fire. *Cement and Concrete Research, 34*(6), 1001-1005.

Li, W., Wang, T., & Han, L.-H. (2019). Seismic performance of concrete-filled double-skin steel tubes after exposure to fire: Experiments. *Journal of Constructional Steel Research, 154*, 209-223.

Li, X., Li, Z., Onofrei, M., Ballivy, G., & Khayat, K. H. (1999). Microstructural characteristics of HPC under different thermo-mechanical and thermo-hydraulic conditions. *Materials and structures, 32*(10), 727-733.

Li, Z., Xu, J., & Bai, E. (2012). Static and dynamic mechanical properties of concrete after high temperature exposure. *Materials Science and Engineering: A, 544*, 27-32.

Lin, W.-M., Lin, T., & Powers-Couche, L. (1996). Microstructures of fire-damaged concrete. *Materials Journal, 93*(3), 199-205.

Ling, T.-C., Poon, C.-S., & Kou, S.-C. (2012). Influence of recycled glass content and curing conditions on the properties of self-compacting concrete after exposure to elevated temperatures. *Cement and Concrete composites, 34*(2), 265-272. doi:https://doi.org/10.1016/j.cemconcomp.2011.08.010

Liu, M. (2011). Incorporating ground glass in self-compacting concrete. *Construction and Building Materials, 25*(2), 919-925.

López-Buendía, A. M., Romero-Sánchez, M. D., Climent, V., & Guillem, C. (2013). Surface treated polypropylene (PP) fibres for reinforced concrete. *Cement and Concrete Research, 54*, 29-35.

Lopez, V., Llamas, B., Juan, A., Moran, J., & Guerra, I. (2007). Eco-efficient concretes: impact of the use of white ceramic powder on the mechanical properties of concrete. *Biosystems engineering, 96*(4), 559-564.

Matesová, D., Bonen, D., & Shah, S. P. (2006). Factors affecting the resistance of cementitious materials at high temperatures and medium [0] heating rates. *Materials and structures, 39*(4), 455-469.

Medina, C., de Rojas, M. I. S., & Frías, M. (2013). Freeze-thaw durability of recycled concrete containing ceramic aggregate. *Journal of Cleaner Production, 40*, 151-160.

Medina, C., Sánchez de Rojas, M. I., & Frías, M. (2012). Reuse of sanitary ceramic wastes as coarse aggregate in eco-efficient concretes. *Cement and Concrete composites, 34*(1), 48-54. oi:https://doi.org/10.1016/j.cemconcomp.2011.08.015

Mujib, S., Md, J., Pal, A., Ibrahim, I., & Mustafy, T. (2022). Numerical Modelling of Concrete-Filled Steel Tube Columns Under Eccentric Loading. Paper presented at the Proceedings of the 5th International Conference on Sustainable Civil Engineering Structures and Construction Materials (pp. 221-240).

Mujib, J. M. S., Shuvo, N. A., Ishmam, A. B. S., & Mustafy, T. (2022). High Temperature Performance of Concrete Incorporating Recycled Glass Powders. Paper presented at the Proceedings of the 5th International Conference on Sustainable Civil Engineering Structures and Construction Materials (pp. 391-403).

Mujib, J. M., Hasan, M., Rasel Molla, M., Zahid, T. M., & Mustafy, T. (2022). Investigation on Fire Resistance of Concrete Incorporating Recycled Ceramic Fine Aggregate. Paper presented at the Proceedings of the 5th International Conference on Sustainable Civil Engineering Structures and Construction Materials (pp. 417-434).

Mustafy, T., & Ahsan, R. (2010, August). FE modeling and experimental verification of a CFRP strengthened steel section subjected to transverse end bearing force. Paper presented at the IABSE-JSCE Joint Conference on Advances in Bridge Engineering-II, August (pp. 8-10).

Mustafy, T., Pal, A., Islam, M., & Ahsan, R. Development of plastic hinge length expression for fiber reinforced polymer strengthened concrete bridge pier. Paper presented at the IABSE-JSCE Joint Conference on Advances in Bridge Engineering-IV, August 26-27, 2020, Dhaka, Bangladesh.

Oliveira, R., de Brito, J., & Veiga, R. (2015). Reduction of the cement content in rendering mortars with fine glass aggregates. *Journal of Cleaner Production, 95*, 75-88.

Özkan, Ö., & Yüksel, İ. (2008). Studies on mortars containing waste bottle glass and industrial by-products. *Construction and Building Materials, 22*(6), 1288-1298.

Pacheco-Torgal, F., & Jalali, S. (2010). Reusing ceramic wastes in concrete. *Construction and Building Materials, 24*(5), 832-838.

Park, S. B., Lee, B. C., & Kim, J. H. (2004). Studies on mechanical properties of concrete containing waste glass aggregate. *Cement and Concrete Research, 34*(12), 2181-2189.

Peng, G., Chan, S. Y. N., Yan, J., Liu, Y., & Yi, Q. (2005). Characteristics of crack growth in high performance concrete subjected to fire. *Journal of Materials Science and Technology, 21*(1), 118-122.

Phan, L. T., & Carino, N. J. (2000). Fire performance of high strength concrete: research needs *Advanced Technology in Structural Engineering* (pp. 1-8).

Poon, C.-S., Azhar, S., Anson, M., & Wong, Y.-L. (2003). Performance of metakaolin concrete at elevated temperatures. *Cement and Concrete composites, 25*(1), 83-89.

Ramezanianpour, A., Esmaeili, M., Ghahari, S.-A., & Najafi, M. (2013). Laboratory study on the effect of polypropylene fiber on durability, and physical and mechanical characteristic of concrete for application in sleepers. *Construction and Building Materials, 44*, 411-418.

Rashid, K., Hameed, R., Ahmad, H. A., Razzaq, A., Ahmad, M., & Mahmood, A. (2018). Analytical framework for value added utilization of glass waste in concrete: Mechanical and environmental performance. *Waste Management, 79*, 312-323.

Raval, A. D., Patel, D., & Pitroda, P. (2013). Ceramic waste: Effective replacement of cement for establishing sustainable concrete. *International Journal of Engineering Trends and Technology (IJETT), 4*(6), 2324-2329.

Salem, Z. T. A., Khedawi, T. S., Baker, M. B., & Abendeh, R. (2017). Effect of waste glass on properties of asphalt concrete mixtures. *Jordan Journal of Civil Engineering, 11*(1).

Sarker, P. K., Kelly, S., & Yao, Z. (2014). Effect of fire exposure on cracking, spalling and residual strength of fly ash geopolymer concrete. *Materials & Design, 63*, 584-592.

Schwarz, N., Cam, H., & Neithalath, N. (2008). Influence of a fine glass powder on the durability characteristics of concrete and its comparison to fly ash. *Cement and Concrete composites, 30*(6),486-496.

Senthamarai, R., Manoharan, P. D., & Gobinath, D. (2011). Concrete made from ceramic industry waste: Durability properties. *Construction and Building Materials, 25*(5), 2413-2419.

Serrano, R., Cobo, A., Prieto, M. I., & de las Nieves González, M. (2016). Analysis of fire resistance of concrete with polypropylene or steel fibers. *Construction and Building Materials, 122*, 302-309.

Shao, Y., Lefort, T., Moras, S., & Rodriguez, D. (2000). Studies on concrete containing ground waste glass. *Cement and Concrete Research, 30*(1), 91-100.

Shi, C., Wu, Y., Riefler, C., & Wang, H. (2005). Characteristics and pozzolanic reactivity of glass powders. *Cement and Concrete Research, 35*(5), 987-993. doi:https://doi.org/10.1016/j.cemconres.2004.05.015

Short, N., Purkiss, J., & Guise, S. (2001). Assessment of fire damaged concrete using colour image analysis. *Construction and Building Materials, 15*(1), 9-15.

Son, K. S., Hajirasouliha, I., & Pilakoutas, K. (2011). Strength and deformability of waste tyre rubber-filled reinforced concrete columns. *Construction and Building Materials, 25*(1), 218-226.

Standard, A. (2015). C143, ASTM International, West Conshohocken, PA. *Standard Test Method for Slump of Hydraulic-Cement Concrete*.

Standard, A. (2016). C187, Standard Test Method for Amount of Water Required for Normal Consistency of Hydraulic Cement Paste. *ASTM International, West Conshohocken, PA*.

Sukontasukkul, P., & Wiwatpattanapong, S. (2009). Moderate lightweight concrete mixed with recycled crumb rubber. *Thammasat Int. J. Sc. Tech, 14*(1), 1-9.

Terro, M. J. (2006). Properties of concrete made with recycled crushed glass at elevated temperatures. *Building and Environment, 41*(5), 633-639. doi:https://doi.org/10.1016/j.buildenv.2005.02.018

Topcu, I. B., & Canbaz, M. (2004). Properties of concrete containing waste glass. *Cement and Concrete Research, 34*(2), 267-274.

Topçu, İ. B., & Canbaz, M. (2004). Properties of concrete containing waste glass. *Cement and Concrete Research, 34*(2), 267-274. doi:https://doi.org/10.1016/j.cemconres.2003.07.003

Torkittikul, P., & Chaipanich, A. (2010). Utilization of ceramic waste as fine aggregate within Portland cement and fly ash concretes. *Cement and Concrete composites, 32*(6), 440-449. doi:https://doi.org/10.1016/j.cemconcomp.2010.02.004

Wang, X.-S., Wu, B.-S., & Wang, Q.-Y. (2005). Online SEM investigation of microcrack characteristics of concretes at various temperatures. *Cement and concrete research, 35*(7), 1385-1390.

Westerholm, M., Lagerblad, B., Silfwerbrand, J., & Forssberg, E. (2008). Influence of fine aggregate characteristics on the rheological properties of mortars. *Cement and Concrete Composites, 30*(4), 274-282.

Zega, C. J., & Di Maio, A. A. (2009). Recycled concrete made with different natural coarse aggregates exposed to high temperature. *Construction and Building Materials, 23*(5), 2047-2052.